Article

Metabolic Modification of *Escherichia coli* BL21 (DE3) to Produce Shinorine

Wanci Wang †, Lingyu Hou †, Jiajia Zhao, Yanyu Qiao, Kuncan Wei, Ding Li, Xiyao Liu *, Yongguang Jiang *

Posted Date: 27 April 2026

doi: 10.20944/preprints202604.1832.v1

Keywords: metabolic engineering; shinorine; *Escherichia coli*; pentose phosphate pathway; genetic engineering

 doi:10.20944/preprints202604.1832.v1

Article

Metabolic Modification of *Escherichia coli* BL21 (DE3) to Produce Shinorine

Wanci Wang [1,†], Lingyu Hou [1,2,†], Jiajia Zhao [1], Yanyu Qiao [1], Kuncan Wei [3], Ding Li [3], Xiyao Liu [4,*] and Yongguang Jiang [1,*]

[1] School of Environmental Studies, China University of Geosciences (Wuhan),Wuhan, China
[2] School of Environmental Science and Engineering, Huazhong University of Science and Technology, Wuhan, China
[3] College of Marine Sciences, Ningde Normal University, Ningde 352100, China
[4] Fujian Provincial Key Laboratory of Featured Biochemical and Chemical Materials, College of New Energy and Materials, Ningde Normal University, Ningde 352100, China
* Correspondence: jiangyg@cug.edu.cn (Y.J.); t1930@ndnu.edu.cn (X.L.)
† These authors have contributed equally to this work.

Abstract

Shinorine, a naturally occurring UV-absorbing compound belonging to the class of mycosporine-like amino acids (MAAs), has attracted considerable attention for its applications in pharmaceuticals, cosmetics, and biomaterials. However, conventional production methods based on extraction from marine organisms are constrained by low yield, limited availability, and environmental sustainability concerns. In this study, we developed a microbial cell factory for the efficient biosynthesis of shinorine in *Escherichia coli*. Specifically, the transaldolase gene in the pentose phosphate pathway (PPP) was precisely disrupted to block the metabolic conversion of sedoheptulose-7-phosphate (S7P), thereby enhancing its intracellular accumulation. In parallel, a cyanobacterial shinorine biosynthetic gene cluster (*Ava_3858–Ava_3855*) was heterologously expressed in the engineered strain, enabling the reconstruction of a functional biosynthetic pathway utilizing S7P as a key precursor. This integrated metabolic engineering strategy effectively overcomes the limitations of traditional extraction methods and significantly improves shinorine production. Moreover, the approach provides a versatile framework for the microbial synthesis of other high-value natural products, with broad implications for sustainable biomanufacturing.

Keywords: metabolic engineering; shinorine; *Escherichia coli*; pentose phosphate pathway; genetic engineering

1. Introduction

In recent years, advances in metabolic engineering and synthetic biology have enabled the heterologous production of natural products, providing a promising strategy for the scalable synthesis of high-value compounds. Shinorine, a representative mycosporine-like amino acid (MAA) produced by marine organisms, exhibits strong ultraviolet (UV) absorption and antioxidant properties, making it highly attractive for applications in pharmaceuticals, cosmetics, and health products[1]. To achieve efficient biosynthesis of shinorine, heterologous expression systems have been successfully established in *Escherichia coli* through metabolic pathway engineering and the introduction of exogenous gene clusters. This strategy typically involves targeted regulation of the host's pentose phosphate pathway (PPP), such as disruption of transaldolase genes to block competing metabolic fluxes and promote the intracellular accumulation of sedoheptulose-7-phosphate (S7P), a key precursor for shinorine biosynthesis. In parallel, the shinorine biosynthetic gene cluster derived from Anabaena variabilis is cloned and heterologously expressed to reconstruct the complete biosynthetic pathway[1]. Together, these approaches enable efficient and scalable

 doi:10.20944/preprints202604.1832.v1

production of shinorine and provide a general framework for microbial synthesis of high-value natural products.

Gene editing technologies based on the λ-Red homologous recombination system offer a rapid and precise method for genetic modification in *E. coli*. This system enables efficient deletion or replacement of target genes, significantly simplifying experimental procedures and improving editing efficiency[2].Gene knockout strategies are widely used to investigate gene function and metabolic regulation, and they also play a critical role in synthetic biology and industrial strain engineering by redirecting metabolic fluxes toward desired products[3].

Transaldolase (Tal1), a key enzyme in the non-oxidative branch of the PPP, plays an essential role in regulating carbon flux distribution. It catalyzes the transfer of a dihydroxyacetone moiety from sedoheptulose-7-phosphate (S7P) to glyceraldehyde-3-phosphate (G3P), generating erythrose-4-phosphate (E4P) and fructose-6-phosphate (F6P)[4]. Previous studies have demonstrated that deletion of Tal1 leads to significant accumulation of S7P, thereby enhancing the biosynthesis of downstream metabolites. For example, in Saccharomyces cerevisiae, Tal1 deletion resulted in an approximately ninefold increase in shinorine production compared to the wild-type strain[4,5]. In contrast, deletion of its homolog NQM1 showed negligible effects, indicating that Tal1 is the primary regulator of S7P metabolism[6]. These findings suggest that Tal1 is a critical control point for precursor availability in shinorine biosynthesis. Based on this insight, the present study aimed to enhance S7P accumulation in *E. coli* by disrupting the *tal1* gene using gene knockout strategies. This modification blocks the conversion of S7P into competing metabolic pathways, thereby increasing intracellular precursor levels for shinorine production.

Currently, shinorine production primarily relies on extraction from marine organisms such as cyanobacteria and red algae. However, this approach is limited by low yield, long production cycles, environmental dependence, and potential ecological risks associated with large-scale harvesting[7,8]. To overcome these limitations, heterologous expression of shinorine biosynthetic genes has been successfully achieved in model organisms such as *E. coli* and yeast [9,10], providing a promising strategy for scalable production of mycosporine-like amino acids (MAAs).

Genomic analysis of Anabaena variabilis ATCC 29413 revealed that the shinorine biosynthetic gene cluster is approximately 6.5 kb in length and consists of four key functional genes (*Ava_3855–3858*)[9]. hese genes encode enzymes responsible for the stepwise synthesis of shinorine. Specifically, *Ava_3858* encodes demethylated 4-deoxygadusol synthase (DDGS), which catalyzes the formation of 4-deoxygadusol (4DG) from sedoheptulose-7-phosphate (S7P). *Ava_3857* encodes an O-methyltransferase (O-MT) involved in 4DG modification. *Ava_3856* encodes an ATP-grasp ligase that catalyzes the condensation of 4DG with glycine to form mycosporine-glycine (MG), while *Ava_3855* encodes a non-ribosomal peptide synthetase (NRPS) that catalyzes the final condensation of MG with serine to produce shinorine. Through this pathway, S7P is sequentially converted into shinorine via intermediate metabolites, with DDGS playing a critical role in initiating precursor formation. Owing to its strong UV absorption (maximum absorption at 260–310 nm) and antioxidant activity, shinorine has been widely applied in sunscreen formulations and medical UV-protective materials[11]. Its ability to scavenge free radicals and mitigate photoaging further highlights its potential as a high-value bioactive compound in cosmetic and pharmaceutical applications [10,12].

To address these challenges, this study constructed a recombinant *E. coli* strain by integrating the MAA biosynthetic gene cluster into the pET29b vector and simultaneously knocking out endogenous transaldolase genes. This combined strategy enhances precursor supply and enables efficient heterologous production of shinorine.

Overall, this work provides a feasible and scalable approach for microbial production of MAAs and offers a valuable reference for reducing production costs through metabolic engineering.

2. Results

2.1. E. Coli BL21 (DE3) Knockout

 doi:10.20944/preprints202604.1832.v1

In this experiment, λ -red homologous recombination system was used to express recombinase through pkd46 plasmid, which mediated homologous recombination of foreign DNA fragments and target genes, so as to knock down the transaldolase gene in *E. coli*, and obtain BL21 (DE3) knockout strain Δ *tala* Δ *talb* (Figure 1).

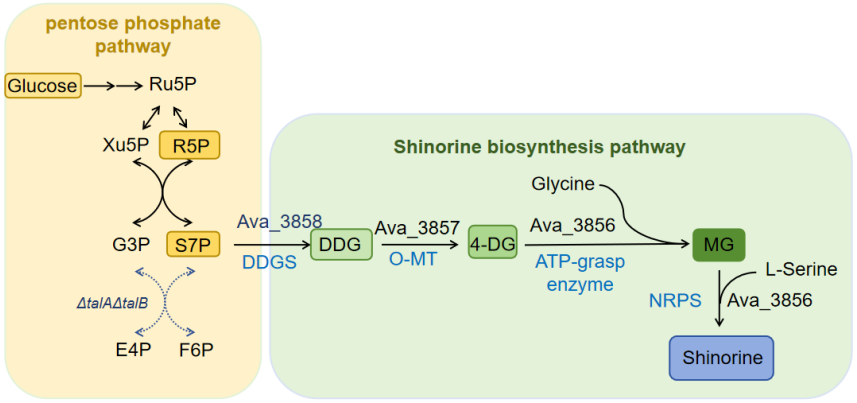

Figure 1. Biological synthesis pathway of shinorine.

2.2. Construction of Recombinant Plasmid of Pet29b Vector

A recombinant plasmid containing the shinorine biosynthetic genes (*Ava_3855_3858*) [9] was constructed using the pET-29b vector and introduced into the previously obtained mutant strain. The ligation order is shown in Figure 2. Successful construction of the recombinant plasmid was verified by sequencing, and a knockout strain carrying the shinorine gene cluster was ultimately obtained.

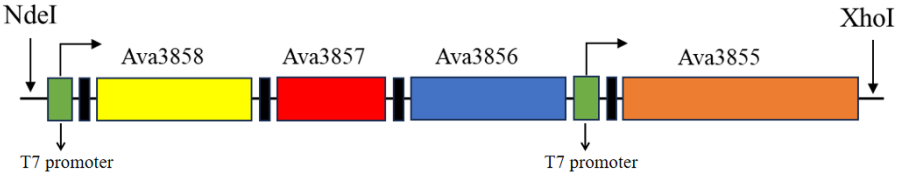

Figure 2. Expression framework of recombinant plasmids.

2.3. Induction and Expression of Recombinant Plasmids

The shinorine biosynthetic gene cluster derived from Anabaena variabilis ATCC 29413 was successfully introduced into *E. coli* for heterologous expression. The gene cluster (~6.5 kb) contains four key functional genes (*Ava_3855–3858*), encoding enzymes involved in the stepwise synthesis of shinorine (Figure 1). Specifically, *Ava_3858* encodes demethylated 4-deoxygadusol synthase (DDGS), which catalyzes the formation of the key intermediate 4-deoxygadusol (4DG) from sedoheptulose-7-phosphate (S7P). *Ava_3857* encodes an O-methyltransferase (O-MT) responsible for 4DG modification. *Ava_3856* encodes an ATP-grasp ligase that catalyzes the condensation of 4DG with glycine to form mycosporine-glycine (MG), while *Ava_3855* encodes a non-ribosomal peptide synthetase (NRPS) that facilitates the final condensation of MG with serine to produce shinorine.

Following IPTG induction, recombinant strains expressing the complete biosynthetic pathway were obtained, indicating successful construction and expression of the heterologous gene cluster. The reconstructed pathway enabled the conversion of intracellular S7P into shinorine via the sequential enzymatic reactions described above.

2.4. Extraction and Yield Optimization of the Product Shinorine

 doi:10.20944/preprints202604.1832.v1

To improve the production yield of shinorine in recombinant *E. coli*, a cultivation strategy combining scale-up fermentation and nutrient optimization was employed across ten experimental groups, including one blank control and nine treatment groups based on orthogonal design parameters. Each group was cultured in a 2-liter aeration bioreactor containing 1 L of glucose-supplemented TB medium. Cultures were aerated and agitated under standard growth conditions, with intermittent supplementation of a concentrated nutrient feed solution to sustain cell growth and metabolic activity throughout the extended cultivation period.The fermentation was carried out continuously for 7 days, the growth level detection of the 7 days is shown in Figure 3. All groups started with an initial OD_{600} of approximately 0.2 on day 0, and the OD_{600} values continuously increased over time, showing a typical logarithmic growth trend of bacterial cultures. By days 6 to 7, the OD_{600} values of all groups approached or reached 20, indicating that the cell density had stabilized and entered the stationary phase. The OD_{600} values of all experimental groups (I–IX) were very close to those of the blank control group at each time point, suggesting that the variables (such as substrates or inducers) had no significant impact on growth, or the differences were minimal under the current conditions.

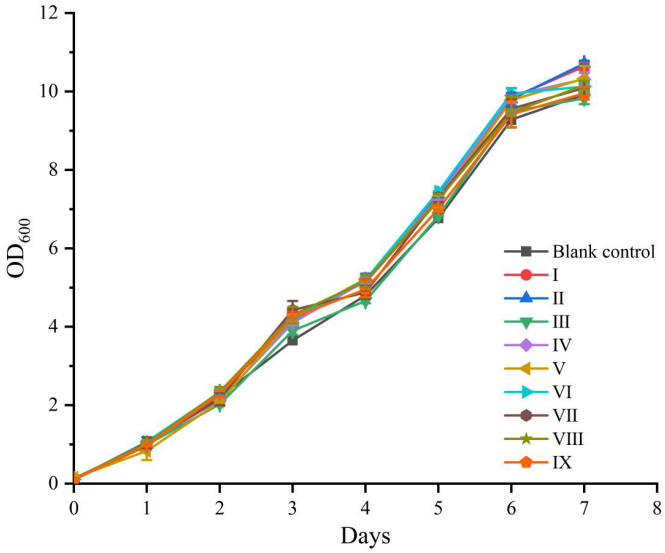

Figure 3. Growth curves for different groups.

To systematically optimize the production conditions for shinorine in recombinant *E. coli*, an orthogonal experimental design approach was employed, focusing on the three most influential factors identified in preliminary studies: glucose concentration, amino acid supplementation (glycine and L-serine), and IPTG induction level. Each factor was tested at three different levels, and an L9(33) orthogonal array was constructed to evaluate nine unique combinations,the composite table is shown in Table 1. This method enables efficient screening of variable interactions while minimizing the number of experiments required.

Table 1. Orthogonal experimental design grouping.

Table 1.1. Experimental factors and levels were defined.

Ingredient	Concentration 1	Concentration 2	Concentration 3
Amino acid(A):	2.5 mM(A1)	5 mM(A2)	10 mM(A3)
Glucose(B):	2 g/L(B1)	5 g/L(B2)	10 g/L(B3)
IPTG(C):	0.5 mM(C1)	1 mM(C2)	1.5 mM(C3)

 doi:10.20944/preprints202604.1832.v1

Table 1.2. The experimental layout based on the $L_9(3^3)$ orthogonal matrix.

Orthogonal experiment group		
Blank control	**0 IPTG, 0 Glucose, 0 Amino acid**	
A1B1C1(I)	A1B2C2(II)	A1B3C3(III)
A2B1C2(IV)	A2B2C3(V)	A2B3C1(VI)
A3B1C3(VII)	A3B2C1(VIII)	A3B3C2(IX)

Following induction and extraction, shinorine production was quantified by HPLC (Figure 4). Significant differences in product yield were observed among the experimental groups. The highest shinorine production reached 2.266 g/L, corresponding to the combination A2B1C2.

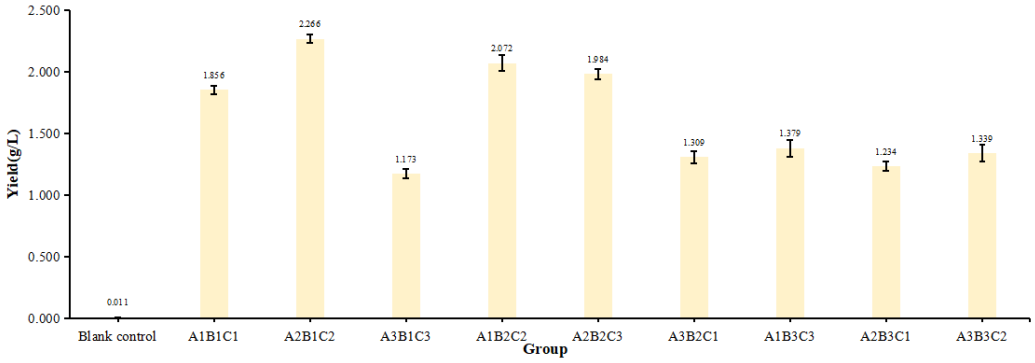

Figure 4. The production of shinorine in each group.

2.4. Effect of Substrate and Induction Conditions on Shinorine Yield

Comparative analysis of all experimental combinations (Figure 5) revealed that shinorine yield was strongly influenced by the tested factors. Range (R) analysis and main effect analysis showed that glucose concentration (Factor B) had the greatest impact on production, followed by amino acid supplementation (Factor A), while IPTG concentration (Factor C) exhibited a comparatively smaller effect.

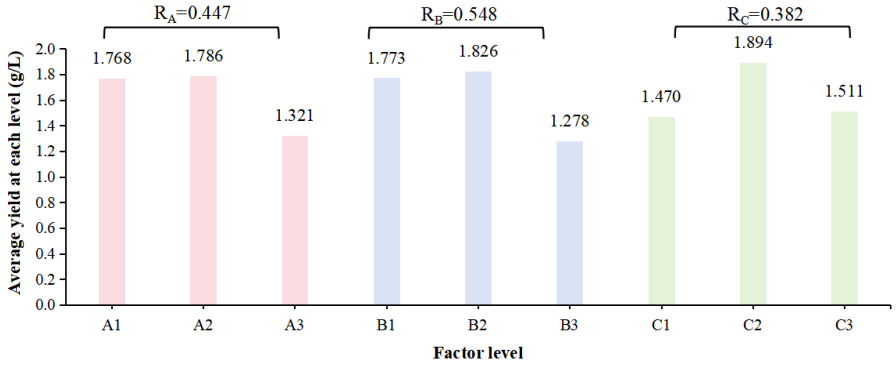

Figure 5. The average yield and the range of each factor at each level. For each factor (A, B, C), calculate the average yield across all experiments at each level and the range R=Max−Min. The yield of the control group was lower than 0.05 g/L.

The optimal condition identified was A2B2C2, corresponding to 2 g/L glucose, 5.0 mM amino acids (glycine and L-serine), and 1 mM IPTG, under which shinorine production reached approximately 2.0 g/L.

Overall, shinorine production varied significantly across different experimental conditions despite similar cell growth profiles. These results indicate that product yield is primarily determined

 doi:10.20944/preprints202604.1832.v1

by metabolic regulation rather than biomass accumulation. The orthogonal experimental design effectively identified key factors influencing production and their relative contributions, providing a basis for further process optimization and scale-up.

2.5. Identification of Shinorine by HPLC–MS

Shinorine production in the recombinant system was confirmed by HPLC–MS analysis (Figure 6). As shown in Figure 6A, a distinct chromatographic peak was observed at a retention time of approximately 1.289 min, indicating the presence of a major compound in the sample. Further identification was performed using mass spectrometry (Figure 6B). The mass spectrum exhibited a dominant ion at m/z 333.13 ($[M+H]^+$), which is consistent with the theoretical molecular weight of shinorine ($C_{13}H_{20}N_2O_8$). In addition, fragment ions at m/z 350.16 and 355.11 were also detected, further supporting the structural assignment.

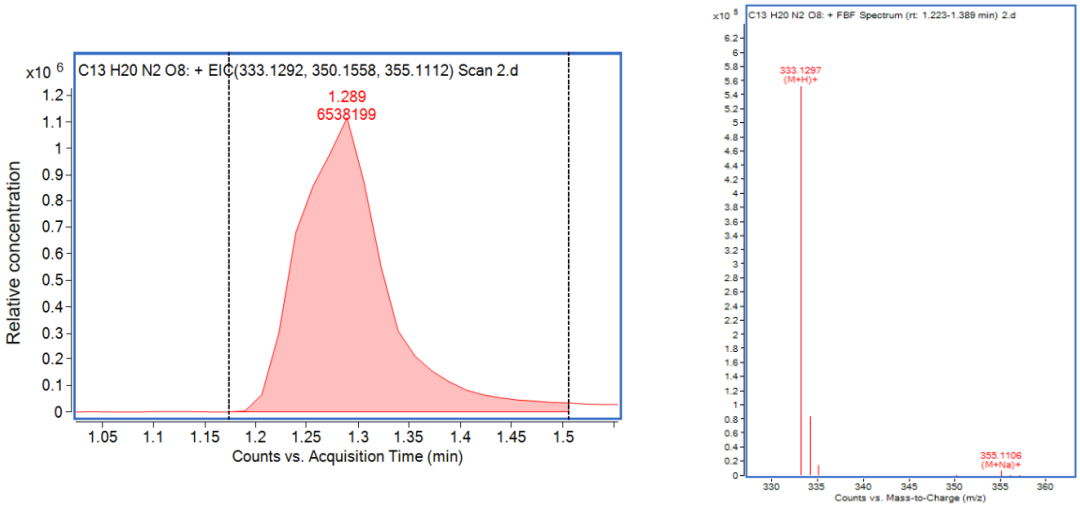

(**a**) (**b**)

Figure 6. Shinorine were tested by HPLC-MS. HPLC analysis of the shinorine (**a**)and fragments of MS1 in the shinorine (**b**).

The agreement between the observed retention time and characteristic mass fragments confirms that the detected compound corresponds to shinorine. These results demonstrate that the engineered strain successfully synthesized shinorine via the reconstructed biosynthetic pathway.

3. Discussion

The successful heterologous production of shinorine in *E. coli* demonstrates the feasibility of reconstructing the complete mycosporine-like amino acid (MAA) biosynthetic pathway in a prokaryotic host. In this study, the integration of the Anabaena variabilis-derived gene cluster (*Ava_3855–3858)* into the engineered ΔtalA ΔtalB strain enabled the effective conversion of intracellular metabolites into shinorine, as confirmed by HPLC–MS analysis. The detection of a characteristic ion at m/z 333.13 ($[M+H]^+$), together with consistent chromatographic behavior, provides strong evidence for successful pathway reconstruction and functional enzyme expression.

A key factor contributing to enhanced shinorine production is the targeted disruption of transaldolase genes (talA and talB). As central enzymes in the non-oxidative pentose phosphate pathway (PPP), transaldolases regulate the interconversion of sugar phosphates and directly influence the availability of sedoheptulose-7-phosphate (S7P), the key precursor for shinorine biosynthesis. Their deletion likely led to the accumulation of S7P, thereby increasing precursor supply and driving metabolic flux toward the heterologous pathway. This result highlights the effectiveness of precursor engineering strategies in improving the production of value-added compounds.

 doi:10.20944/preprints202604.1832.v1

Interestingly, no significant differences in biomass were observed among experimental groups under varying substrate and induction conditions, while shinorine yield varied substantially . This indicates that product formation is decoupled from cell growth and is instead primarily governed by intracellular metabolic flux distribution. Such a phenomenon is commonly observed in engineered microbial systems, where overexpression of heterologous pathways imposes metabolic burden and shifts cellular resources toward product synthesis rather than biomass accumulation.

The orthogonal experimental design further revealed that glucose concentration exerted the most significant influence on shinorine production, followed by amino acid supplementation and IPTG induction level . This finding can be mechanistically explained by the central role of glucose in fueling the PPP, thereby determining the intracellular pool of S7P. Meanwhile, supplementation of glycine and L-serine directly supports downstream condensation reactions catalyzed by ATP-grasp ligase and NRPS, enhancing product formation efficiency. In contrast, IPTG primarily regulates the expression level of pathway enzymes, and excessive induction may lead to metabolic stress or protein misfolding, explaining its relatively lower impact compared to substrate availability.

The optimized condition (A2B2C2) achieved a shinorine yield of approximately 2.0–2.266 g/L, which is comparable to or higher than previously reported microbial production systems. This demonstrates that the combined strategy of metabolic pathway reconstruction and precursor supply optimization is effective for improving MAA biosynthesis in *E. coli*. Moreover, the use of an orthogonal design approach enabled efficient identification of key influencing factors and their interactions, providing a practical framework for process optimization.

Despite these promising results, several limitations remain. First, the accumulation of intermediates and potential metabolic bottlenecks within the pathway were not quantitatively assessed, which may restrict further yield improvement. Second, the balance between precursor supply and enzyme expression requires more precise regulation, potentially through dynamic control strategies or promoter engineering. Future studies could integrate systems biology approaches, such as metabolomics and flux analysis, to further elucidate pathway regulation and enhance production efficiency.

Overall, this study demonstrates a robust strategy for the microbial production of shinorine by combining gene knockout, heterologous pathway reconstruction, and process optimization. These findings provide a valuable foundation for the scalable and sustainable biosynthesis of MAAs and other high-value natural products.

4. Materials and Methods

4.1. E. Coli BL21 (DE3) Knockout

Bacteria, and 100 μl of the transformed DH5α (λ PIR) competent cells were added to LB solid agar medium plate containing ampicillin (50 μg/mL). The plate was placed at room temperature until the liquid was completely absorbed, and then the plate was inverted. After the growth of single bacteria, select a single colony to culture and maintain the seed and expand the culture for 5–10 mL, and extract the high concentration pkd3 plasmid with the Plasmid Extraction Kit [21]. High concentrations of pkd46 and pcp20 helper plasmids were extracted by the same procedure.

Using pkd3 as template, the target fragments with homology arms at both ends of *tala* and *talb* genes were amplified by PCR, providing high concentration DNA fragments for electrotransformation. The pkd46 plasmid was transferred into BL21 (DE3) strain by heat shock, and the species were preserved after resistance screening and PCR verification. After the BL21 (DE3) strain carrying pkd46 was successfully constructed, a high concentration of PCR product was electrotransferred into the induced strain, and the correct structure of the mutant was verified by three sets of PCR: the internal sequence of the target gene was amplified in the first group (AUP and cat-c1 or BUP and cat-c1) to confirm the deletion, the homology arm junction region was amplified in the second group (cat-c2 and adown or cat-c2 and bdown) to ensure the accuracy of the recombination site, and the flanking sequence was amplified in the third group (AUP and adown or BUP and bdown) to exclude nonspecific recombination [22]. The synthesis primers and verification

 doi:10.20944/preprints202604.1832.v1

primers are listed in Supplementary Table 1. After successful verification, the pkd46 plasmid was lost by using the temperature sensitive property, and the BL21 (DE3) mutant strain was further screened by ampicillin resistance detection and PCR. Subsequently, the temperature sensitive plasmid pCP20 was transformed into mutants containing chloramphenicol resistance (CmR) markers, and the ampicillin resistant transformants were screened at 30 ° C. Subsequently, the pcp20 plasmid was cultured at high temperature to promote the loss of the plasmid [23]. Finally, the BL21 (DE3) Δ *tala* knockout strain without exogenous plasmid was obtained by ampicillin sensitivity detection. In the same step, the *talb* gene in BL21 (DE3) Δ *tala* knockout strain was knocked down to obtain BL21 (DE3) Δ *tala* Δ *talb* knockout strain.

4.2. Construction of Recombinant Plasmid of Pet29b Vector

Using the plasmid vector carrying the biosynthetic genes as a template, each fragment of the shinorine biosynthetic genes was amplified with specific primer pairs and purified. The amplified fragments and the vector were then digested with NdeI and XhoI (New England Biolabs) at 37 °C for 2.5 hours, and digestion efficiency was confirmed by DNA gel electrophoresis. Upon successful verification, the purified DNA fragment *Ava3858–3857* was ligated into the linearized pET-29b(+) expression vector using T4 DNA ligase to generate the recombinant plasmid pAva_58-57. Next, the purified *Ava3856* DNA fragment was ligated into pAva_58-57 (digested with the same enzymes) to obtain pAva_58-56. Finally, the purified *Ava3855* fragment was ligated into pAva_58-56, resulting in the final recombinant plasmid pAva_55-58.

4.3. Extraction and Purification of the Product

The recombinant *E. coli* strain harboring the plasmid was first cultured in 100 mL of TB medium at 37 °C until the optical density at 600 nm (OD_{600}) reached 0.5–0.6. At this point, 0.5 mM IPTG was added to induce gene expression. The culture was then transferred to 20 °C and incubated for an additional 20 h to allow for continuous induction. After induction, 10 mL of the culture was collected and centrifuged at 6000 rpm for 15 minutes. Since MAAs are highly soluble in ethanol, the resulting cell pellet was resuspended in 5 mL of 50% methanol. The suspension was subjected to ultrasonic cell disruption in an ice bath using a Fisher Scientific Model 550 ultrasonic homogenizer (20 s pulses, repeated 3 times with 1-min intervals for cooling) to facilitate efficient release of shinorine. The disrupted sample was then centrifuged at 12,000 × g for 10 minutes to remove cell debris. The resulting supernatant, containing the crude shinorine extract, was filtered through a 0.22 μm membrane. The filtrate was subsequently concentrated and purified using an Amicon Ultra 0.5 mL Ultracel 3K centrifugal filter device (Millipore) at 13,300 rpm for 30 minutes. This step effectively reduced interference from proteins and polysaccharides, thereby improving the accuracy of subsequent spectroscopic analyses [24].

4.4. Preparation of Shinorine Standard

We employed a high-yield MAA-producing *E. coli* engineered strain developed in our laboratory for large-scale cultivation and shinorine extraction. The crude extract was first subjected to solid-phase extraction (SPE) to remove impurities. Subsequently, high-performance liquid chromatography (HPLC) was used to isolate shinorine based on its retention time, and the middle fraction corresponding to shinorine was collected. The purified fraction was then lyophilized to obtain shinorine as a standard compound. Finally, the purity of the standard was determined through quantitative analysis, and a standard calibration curve was established for accurate measurement of shinorine content in subsequent samples ($y = 2248.2x + 28878$ $R^2 = 0.999$), the total run time was set to 20 min [25].

 doi:10.20944/preprints202604.1832.v1

4.5. Product Identification

The crude shinorine extract obtained in the previous step was subjected to HPLC analysis. The chromatographic analysis was performed using a Synergi 4μ Fusion-RP C18 80A column (250 × 4.6 mm, Phenomenex), equipped with an RP-8 guard column. The mobile phase consisted of 50% methanol and 0.2% chromatographic-grade acetic acid, designated as phases A and B, which were isocratically eluted at a 1:1 ratio. The flow rate was set to 0.5 mL/min, with detection at 333 nm. The column temperature was maintained at 30 °C, the injection volume was 20 μL, and the total run time was set to 20 min [25].

Additionally, analysis was performed using a Waters Acquity UPLC H-Class system coupled with a Xevo Triple Quadrupole Mass Spectrometer (Ireland). The chromatographic separation was conducted using a Waters Acquity UPLC BEH C18 column (2.1 × 50 mm, 1.7 μm particle size). LC conditions were as follows: the column temperature was maintained at 40 °C; the mobile phases consisted of 0.1% formic acid in methanol and 0.1% formic acid aqueous solution, with isocratic elution at a flow rate of 200 μL/min. The injection volume was 10 μL, and the total run time was 30 min. For mass spectrometry conditions, electrospray ionization (ESI) in positive ion mode was employed. The source temperature was set to 150 °C, and the desolvation (spray) temperature was 450 °C. The capillary voltage was 3.0 kV, and the cone voltage was 5 V. Argon was used as the collision gas, while nitrogen served as both the desolvation and cone gases. The respective gas flow rates were 0.2 mL/min (argon), 650 L/h (desolvation gas), and 20 L/h (cone gas).The HPLC chromatogram and the primary mass spectrum are shown in Figure 3. It was found that the two most prominent fragment peaks in the primary mass spectrum appeared at m/z 333.13 and 355.11. Notably, the first peak at m/z 333.13 is consistent with the fragment ion reported for shinorine in the literature [26].

4.6. Optimization of Substrates and Inducers

The efficient biosynthesis of shinorine in recombinant *E. coli* systems relies heavily on the availability and balance of specific metabolic precursors and the appropriate regulation of gene expression [5]. Glucose serves as the primary carbon source and is essential for the generation of key intermediates through the pentose phosphate pathway (PPP). In particular, sedoheptulose-7-phosphate (S7P), a central PPP intermediate, is a direct precursor for the synthesis of 4-deoxygadusol (DDG), the core chromophore scaffold in shinorine biosynthesis [9]. Enhanced glucose availability has been shown to increase intracellular flux through the PPP, thereby promoting DDG production [27]. However, excessive glucose concentrations may lead to metabolic burden or overflow metabolism, which can inhibit cell growth and recombinant protein expression [28]. Thus, glucose levels must be finely optimized to balance cell health with precursor supply. And shinorine biosynthesis involves condensation reactions between DDG and nitrogenous substrates, typically facilitated by non-ribosomal peptide synthetase (NRPS)-like enzymes encoded by the gene cluster (*Ava_3855–3858*) [9]. Two critical amino acid precursors in this process are glycine and L-serine. These amino acids serve as donors of amino groups and side chains for the formation of intermediate molecules such as mycosporine-glycine (MG), which is subsequently amidated to form shinorine. Studies have shown that external supplementation of glycine and serine can significantly enhance product yield, especially in engineered systems where native amino acid biosynthesis pathways are insufficient to meet the demand imposed by high-level expression of the biosynthetic genes [29,30].

The shinorine biosynthetic pathway is typically introduced into *E. coli* under the control of an IPTG-inducible promoter (T7 systems). Isopropyl β-D-1-thiogalactopyranoside (IPTG) serves as a molecular inducer that binds to the lac repressor and activates transcription of the target genes, enabling production of pathway enzymes such as 4-deoxygadusol synthase and NRPS-like enzymes [31]. The timing, concentration, and duration of IPTG induction are crucial parameters that impact overall protein expression and metabolic flux. Premature induction can result in metabolic stress, while excessive IPTG levels may lead to inclusion body formation or cytotoxicity [32]. Empirical

 doi:10.20944/preprints202604.1832.v1

optimization has suggested that moderate IPTG concentrations (1 mM) and induction at mid-log phase (OD600 ≈ 0.5–0.6) strike a balance between enzyme expression and cellular viability [33].

5. Conclusions

In this study, an engineered *E. coli* strain was successfully constructed for the efficient biosynthesis of shinorine, a mycosporine-like amino acid (MAA) with excellent UV-absorbing and antioxidant properties [7,8]. The engineered strain achieved a maximum shinorine yield of 2.266 g/L, and the optimized strain has the potential to achieve even higher yields. Representing a substantial improvement over yields obtained via traditional extraction from marine organisms such as cyanobacteria and red algae [10,11] (Table 2). Conventional methods suffer from significant limitations, including restricted raw material availability, seasonal variability, low extraction efficiency, and difficulties in purification due to the coexistence of structurally similar MAAs. Typically, only 1–3 g of pure MAAs can be obtained from one ton of biomass, making industrial-scale application impractical [10].

Table 2. Comparison of shinorine yields from different sources.

Host	Yield	Reference
Synechocystis sp.	2.37 mg/L	(Yang G et al. 2018) [13]
M. alcaliphilum	17.1 mg/L	(Nguyen AD et al. 2020) [14]
Corynebacterium. glutamicum	19 mg/L	(Wei L et al. 2019) [15]
Streptomyces avermitilis	154 mg/L	(Miyamoto KT et al. 2014) [16]
Y. lipolytica	207 mg/L	(Jin H et al. 2023) [17]
P. putida	900 mg/L	(Yunus IS et al. 2024) [18]
Escherichia coli	1.2 g/L	(De Leeuw M et al. 2023) [19]
Saccharomyces. cerevisiae	1.6 g/L	(Kim S et al. 2023) [20]
Escherichia coli BL21(DE3)	2.266 g/L	————

Through systematic metabolic engineering, we successfully established a robust microbial cell factory for shinorine production. Key optimization strategies were implemented to overcome biosynthetic bottlenecks. Specifically, deletion of the transaldolase gene in the pentose phosphate pathway (PPP) led to enhanced accumulation of sedoheptulose-7-phosphate (S7P), a key precursor [4,5]. In addition, a dynamic regulation strategy was applied to decouple cell growth and product accumulation by inducing MAA biosynthesis at the late growth stage [34]. This approach effectively mitigated the resource competition between biomass formation and secondary metabolite production, resulting in an order-of-magnitude increase in MAA yield.

This study demonstrates that precise modulation of the pentose phosphate pathway (PPP) represents a key strategy for enhancing the biosynthetic efficiency of mycosporine-like amino acids (MAAs), primarily through the redirection of intracellular carbon flux toward the accumulation of the critical precursor sedoheptulose-7-phosphate (S7P). Furthermore, synergistic multi-gene engineering was shown to exert multiplicative effects on metabolic flux redistribution and final product titers [35], highlighting the importance of coordinated pathway optimization rather than single-gene interventions. Compared to conventional extraction from marine organisms, microbial biosynthesis offers substantial advantages in terms of yield, cost-effectiveness, process controllability, and product purity. In this context, the metabolic engineering framework developed in this study not only enables efficient production of shinorine in *E. coli*, but also provides a broadly applicable platform for the biosynthesis of other MAAs and structurally related high-value natural products.

Notably, this work underscores the critical role of precursor supply regulation and pathway reconstruction in overcoming intrinsic metabolic bottlenecks, thereby advancing the development of robust microbial cell factories. The successful implementation of shinorine biosynthesis further illustrates the potential of synthetic biology to replace traditional resource-intensive production methods with more sustainable and scalable alternatives. Future efforts should focus on enhancing

 doi:10.20944/preprints202604.1832.v1

strain robustness and metabolic stability under industrial fermentation conditions, as well as optimizing redox balance and cofactor availability to further improve production efficiency. Exploration of non-conventional microbial hosts and co-culture systems may provide additional opportunities for process intensification and scalability. Moreover, expanding this platform toward the co-production of structurally diverse MAAs or other UV-protective compounds could significantly increase its industrial relevance. Finally, the integration of emerging tools such as machine learning-guided pathway design, adaptive laboratory evolution, and systems-level omics analysis is expected to further refine metabolic control and unlock new frontiers in microbial production performance, paving the way for environmentally sustainable and economically viable biomanufacturing of natural sunscreens and related bioactive compounds [36,37].

Author Contributions: Conceptualization, Y.J. and X.L. ; methodology, W.W. and L.H.; validation, W.W., L.H. and J.Z.; formal analysis, W.W.; investigation, W.W., L.H., J.Z., K.W. and Y.Q.; resources, D.L., X.L. and Y.J.; data curation, W.W.; writing—original draft preparation, W.W. and L.H.; writing—review and editing, D.L., X.L. and Y.J.; visualization, W.W.; supervision, D.L., X.L. and Y.J.; project administration, D.L. and Y.J.; funding acquisition, Y.J. and X.L. All authors have read and agreed to the published version of the manuscript.

Funding: This research was funded by the National Key Research and Development Program of "Synthetic Biology" of the Ministry of Science and Technology, 2018YFA0901300, "Design and Enhancement of Bidirectional Electron Transfer System for Electric Energy Cells", Yongguang Jiang, and the Scientific Research Foundation of Ningde Normal University (2025HX11) , Xiyao Liu.

Conflicts of Interest: The authors declare no conflicts of interest.

References

1. Hengardi MT, Liang C, Madivannan K, et al. Reversing the directionality of reactions between non-oxidative pentose phosphate pathway and glycolytic pathway boosts mycosporine-like amino acid production in Saccharomyces cerevisiae. Microb Cell Fact. 2024;23(1):121. Published 2024 May 9.
2. Pósfai G, Plunkett G 3rd, Fehér T, et al. Emergent properties of reduced-genome *Escherichia coli*.Science. 2006;312(5776):1044-1046.
3. Sharan SK, Thomason LC, Kuznetsov SG, Court DL. Recombineering: a homologous recombination-based method of genetic engineering. Nat Protoc. 2009;4(2):206-223.
4. Kruger, N. J., & von Schaewen, A. The oxidative pentose phosphate pathway: structure and organisation. Current Opinion in Plant Biology, 2003, 6(3), 236–246.
5. Zhao, J., Li, Q., Sun, T., Zhu, X., Xu, H., & Ma, Y. Engineering central metabolic modules of *Escherichia coli* for improving shikimic acid production. Microbial Cell Factories, 2019, 18(1), 1–14.
6. Yoshida, S., Tsunematsu, Y., Tanaka, M., & Watanabe, K. Engineering of pentose phosphate pathway to improve production of aromatic compounds in yeast. Journal of Bioscience and Bioengineering, 2015, 119(1), 12–17.
7. Shick, J. M., & Dunlap, W. C. Mycosporine-like amino acids and related gadusols: biosynthesis, accumulation, and UV-protective functions in aquatic organisms. Annual Review of Physiology, 2002, 64, 223–262.
8. Rastogi RP, Sinha RP, Moh SH, Lee TK, Kottuparambil S, Kim YJ, Kang JW, Han T. Mycosporine-like amino acids (MAAs): photoprotective compounds and their prospects in the global cosmeceutical market. Environ Sci Biotechnol. 2010, 9(3):197-223.
9. Balskus, E. P., & Walsh, C. T. The genetic and molecular basis for sunscreen biosynthesis in cyanobacteria. Science, 2010, 329(5999), 1653–1656.
10. Sinha, R. P., & Häder, D. P. UV-protectants in cyanobacteria. Plant Science, 2007, 174(3), 278–289.
11. de la Coba, F., Aguilera, J., Figueroa, F. L., de Gálvez, M. V., & Herrera, E.Antioxidant activity of mycosporine-like amino acids isolated from three red macroalgae and one marine lichen. Journal of Applied Phycology, 2009, 21(2), 161–169.

 doi:10.20944/preprints202604.1832.v1

12. Rastogi, R. P., & Incharoensakdi, A. UV radiation-induced biosynthesis, stability and antioxidant activity of mycosporine-like amino acids (MAAs) in a unicellular cyanobacterium Gloeocapsa sp. CU2556. Journal of Photochemistry and Photobiology B: Biology, 2014, 130, 287–292.
13. Yang G, Cozad MA, Holland DA, Zhang Y, Luesch H, Ding Y. Photosynthetic Production of Sunscreen Shinorine Using an Engineered Cyanobacterium.ACS Synth Biol. 2018;7(2):664-671.
14. Nguyen A D , Tin C H T , Lee E Y .Methanotrophic microbial cell factory platform for simultaneous conversion of methane and xylose to value-added chemicals[J].Chemical Engineering Journal, 2020.
15. Wei L, Wang H, Xu N, et al. Metabolic engineering of Corynebacterium glutamicum for L-cysteine production.Appl Microbiol Biotechnol. 2019;103(3):1325-1338.
16. Miyamoto KT, Komatsu M, Ikeda H. Discovery of gene cluster for mycosporine-like amino acid biosynthesis from Actinomycetales microorganisms and production of a novel mycosporine-like amino acid by heterologous expression.Appl Environ Microbiol. 2014;80(16):5028-5036.
17. Jin H, Kim S, Lee D, Ledesma-Amaro R, Hahn JS. Efficient production of mycosporine-like amino acids, natural sunscreens, in Yarrowia lipolytica. Biotechnol Biofuels Bioprod. 2023;16(1):162. Published 2023 Oct 29.
18. Yunus I S , Hudson G A , Chen Y ,et al.Systematic engineering for production of anti-aging sunscreen compound in Pseudomonas putida[J].Metabolic Engineering, 2024, 84(000):14.
19. De Leeuw M, Matos MRA, Nielsen LK. Omics data for sampling thermodynamically feasible kinetic models.Metab Eng. 2023;78:41-47.
20. Kim S, Park BG, Jin H, et al. Efficient production of natural sunscreens shinorine, porphyra-334, and mycosporine-2-glycine in Saccharomyces cerevisiae. Metab Eng. 2023;78:137-147.
21. Sambrook, J., & Russell, D. W. Molecular Cloning: A Laboratory Manual (3rd ed.). Cold Spring Harbor Laboratory Press, 2001.
22. Datsenko, K. A., & Wanner, B. L. One-step inactivation of chromosomal genes in *Escherichia coli* K-12 using PCR products. Proceedings of the National Academy of Sciences, 2000，97(12), 6640–6645.
23. Cherepanov, P. P., & Wackernagel, W. Gene disruption in *Escherichia coli*: TcR and KmR cassettes with the option of Flp-catalyzed excision of the antibiotic-resistance determinant. Gene, 1995, 158(1), 9–14. https://doi.org/10.1016/0378-1119(95)00193-A
24. Rastogi R. P., Sonani R. R., Madamwar D., et al., Characterization and antioxidant functions of mycosporine-like amino acids in the cyanobacterium Nostoc sp. R76DM [J]. Algal Research, 2016, 16: 110-118.
25. Liu Z., Häder D. P., and Sommaruga R., Occurrence of mycosporine-like amino acids (MAAs) in the bloom-forming cyanobacterium. Microcystis aeruginosa, Journal of Plankton Research, Volume 26, Issue 8, August 2004, Pages 963–966.
26. Whitehead, K., & Hedges, J. I. Analysis of mycosporine-like amino acids in plankton by liquid chromatography electrospray ionization mass spectrometry. Marine Chemistry, 2002, 80(1), 27–39.
27. Liu, H., Valdehuesa, K. N. G., Nisola, G. M., Ramos, K. R. M., Kim, H. T., Lee, W. K., Chung, W. J., & Park, S. J. Enhancing NADPH availability for microbial production of value-added chemicals through metabolic engineering. Biotechnology Advances, 2020, 44, 107614.
28. Bentley, W. E., Mirjalili, N., Andersen, D. C., Davis, R. H., & Kompala, D. S. Plasmid-encoded protein: the principal factor in the "metabolic burden" associated with recombinant bacteria. Biotechnology and Bioengineering, 1990, 35(7), 668–681.
29. Wu, G., Bazer, F. W., Dai, Z., Li, D., Wang, J., & Wu, Z. Amino acid nutrition in animals: protein synthesis and beyond. Annual Review of Animal Biosciences, 2016, 2, 387–417.
30. Hu, Y., Zhao, L., Wang, J., Yu, X., & Zhang, B. Enhancing non-natural amino acid incorporation in *E. coli* by improving endogenous precursor biosynthesis. Biotechnology Journal, 2022, 17(5), 2100540.
31. Studier, F. W., & Moffatt, B. A. Use of bacteriophage T7 RNA polymerase to direct selective high-level expression of cloned genes. Journal of Molecular Biology, 1986, 189(1), 113–130.
32. Sørensen, H. P., & Mortensen, K. K. Soluble expression of recombinant proteins in the cytoplasm of *Escherichia coli*. Microbial Cell Factories, 2005, 4(1), 1.

 doi:10.20944/preprints202604.1832.v1

33. Rosano, G. L., & Ceccarelli, E. A. Recombinant protein expression in *Escherichia coli*: advances and challenges. Frontiers in Microbiology, 2014, 5, 172.
34. Li C, Bai Y, Zhang H, Zhang J, Liu X, Wang Y. Dynamic regulation strategies for improving microbial synthesis of natural products. Biotechnol Adv. 2022;58:107888.
35. Xu P, Wang X, Jones ZB, Li M, Koffas BS, Koffas MAG. Modular optimization of multi-gene pathways for microbial biosynthesis. Nat Commun. 2020,11:1-12.
36. Carbonell P, Radivojevic T, King RD. Opportunities at the intersection of synthetic biology, machine learning, and automation. ACS Synth Biol. 2019,8(7):1474-1477.
37. Nielsen J, Keasling JD. Engineering cellular metabolism. Cell. 2016,164(6):1185-1197.